CONDENSED MATTER

Thermal Properties of Rare Earth Cobalt Oxides and of $La_{1-x}Gd_xCoO_3$ Solid Solutions

Yu. S. Orlov[a, b]*, V. A. Dudnikov[a], M. V. Gorev[a], S. N. Vereshchagin[c], L. A. Solov'ev[d], and S. G. Ovchinnikov [a, d]

[a] *Kirensky Institute of Physics, Siberian Branch, Russian Academy of Sciences, Akademgorodok, Krasnoyarsk, 660036 Russia*
[b] *Siberian Federal University, Svobodnyi pr. 79, Krasnoyarsk, 660041 Russia*
[c] *Institute of Chemistry and Chemical Technology, Siberian Branch, Russian Academy of Sciences, Akademgorodok, Krasnoyarsk, 660036 Russia*
[d] *National Research Nuclear University MEPhI (Moscow Engineering Physics Institute), Kashirskoe sh. 31, Moscow, 115409 Russia*
* e-mail: jso.krasn@mail.ru
Received March 22, 2016; in final form, April 6, 2016

Powder X-ray diffraction data for the crystal structure, phase composition, and molar specific heat for $La_{1-x}Gd_xCoO_3$ cobaltites in the temperature range of 300−1000 K have been analyzed. The behavior of the volume thermal expansion coefficient in cobaltites with isovalent doping in the temperature range of 100−1000 K is studied. It is found that the $\beta(T)$ curve exhibits two peaks at some doping levels. The rate of the change in the occupation number for the high-spin state of cobalt ions is calculated for the compounds under study taking into account the spin−orbit interaction. With the Birch−Murnaghan equation of state, it is demonstrated that the low-temperature peak in the thermal expansion shifts with the growth of the pressure toward higher temperatures and at pressure $P \sim 7$ GPa coincides with the second peak. The similarity in the behavior of the thermal expansion coefficient in the $La_{1-x}Gd_xCoO_3$ compounds with the isovalent substitution and the undoped $LnCoO_3$ compound (Ln is a lanthanide) is considered. For the whole series of rare earth cobalt oxides, the nature of two specific features in the temperature dependence of the specific heat and thermal expansion is revealed and their relation to the occupation number for the high-spin state of cobalt ions and to the insulator−metal transition is established.

The promising applications of rare earth cobaltites having the general formula $Ln_{1-x}M_xCoO_3$ (Ln is a lanthanide and M is a rare earth or alkaline earth metal) in different technological processes and devices [1−3], as well as their usage as model materials in the analysis of different physical characteristics, have supported a vivid interest in their studies for more than a half century [4−6]. A characteristic feature of cobaltites is the manifestation of multiplicity fluctuations [7] in Co^{3+} resulting in the anomalies in their magnetic, electrical, and structural characteristics. Different spin states of cobalt ions are due to the interplay between the interatomic exchange interaction and the crystal field, which depend on external conditions such as temperature and pressure. As a result, cobalt ions can be in the low-spin (LS, $S = 0$, t_{2g}^6), intermediate-spin (IS, $S = 1$, $t_{2g}^5 e_g^1$), and high-spin (HS, $S = 2$, $t_{2g}^4 e_g^2$) states. The chemical pressure arising at the partial isovalent or complete substitution of one lanthanide for another in $LnCoO_3$ compounds can also play the role of external pressure. Such pressure can lead to either the stabilization or destabilization of the low-spin ground state in Co^{3+} ions depending on the ionic radius of the substituting chemical element. The thermal expansion coefficients of rare earth cobaltites have an unusual temperature dependence [8−10] and can be anomalously large. The additional degrees of freedom related to the multiplicity fluctuations affect also the transport characteristics such as electrical and thermal conductivities and lead to unusually high thermoelectric coefficients of cobaltites [11]. Therefore, the studies of the fascinating properties of nonstoichiometric cobaltites are promising also from the viewpoint of the search for novel thermoelectric materials.

In [12], the coexistence of two types of domains having the same crystal lattice symmetry but differing in the b parameter and the unit cell volume was revealed in the high-precision X-ray diffraction data [12] for $GdCoO_3$ in an intermediate temperature range

Parameters and volumes of the unit cells for polycrystalline $La_{1-x}Gd_xCoO_3$ samples

Composition	V/Z, Å^3	Unit cell parameters, Å
$LaCoO_3$	56.02 trigonal, $Z = 6$	5.44459(2) 13.0931(1)
$La_{0.95}Gd_{0.05}CoO_3$	55.79 trigonal, $Z = 6$	5.43871(7) 13.0675(2)
$La_{0.9}Gd_{0.1}CoO_3$	55.60 trigonal (55%)	5.4337(1) 13.0467(5)
	55.68 orthorhombic (46%)	5.4325(3) 5.3739(3) 7.6301(4)
$La_{0.8}Gd_{0.2}CoO_3$	55.38 orthorhombic, $Z = 4$	5.4151(1) 5.3715(1) 7.6156(2)
$La_{0.5}Gd_{0.5}CoO_3$	54.16 orthorhombic, $Z = 4$	5.3436(10) 5.3611(5) 7.5614(12)
$GdCoO_3$	52.54 orthorhombic, $Z = 4$	5.2256(3) 5.3935(2) 7.4568(1)

(200−700 K). The ab initio DFT-GGA calculations demonstrate that these domains correspond to two possible states of $GdCoO_3$ with HS and LS configurations of Co^{3+}. The calculations also reveal a nontrivial relation of the anomalously high thermal expansion coefficient in $GdCoO_3$ to the spin state changes in Co^{3+} ions. The thermal expansion of the crystal lattice leads to a decrease in the spin gap (energy distance between the low- and high-spin states) and to the growth of the content of the high-spin states. On the other hand, the larger ionic radius of the high-spin Co^{3+} ions gives rise to an additional growth of the volume on heating. As a result, the contribution of multiplicity fluctuations to the thermal expansion coefficient related to the large difference in the ionic radii (about 10%) corresponding to the HS state ($r_{HS} = 0.61$ Å) and LS state ($r_{LS} = 0.545$ Å) is an order of magnitude larger than the usual contribution from anharmonicity. The two-phase model formulated in [12] provides a good qualitative description of the thermal expansion characteristics of $GdCoO_3$, but does not explain the existence of two peaks observed in the temperature dependence of the thermal expansion coefficient of $LnCoO_3$ (Ln = La, Pr, Nd) compounds [8−10].

Our work is aimed at the study of the relation between the multiplicity fluctuations and the structural and thermal anomalies in rare earth cobaltites. With this aim in view, we study the thermal expansion and molar specific heat of $La_{1-x}Gd_xCoO_3$ ($0 \le x \le 1$) rare earth cobaltites with the isovalent substitution within the temperature range of 100−1000 K, calculate the occupation number of the high-spin state, and analyze the obtained data.

The polycrystalline $La_{1-x}Gd_xCoO_3$ ($x = 0−1.0$) samples were prepared using the conventional ceramic technology. High-purity (99.9%) La_2O_3, Gd_2O_3, and Co_3O_4 oxides taken in the stoichiometric proportion were thoroughly mixed in jasper mortar using ethanol. Then, the mixture was annealed in air at 1100°C with the triple repetition of the grinding−calcination cycles. The pressurized pellets were annealed at the same temperature for 24 h and then cooled to room temperature at a rate of 2°C/min.

The X-ray structural and phase analysis was performed using a PANalytical X'Pert PRO (Co K_α) diffractometer over the angular range $2\theta = 10°−140°$. The high-temperature measurement was performed using an Anton Paar HTK 1200N camera. The data processing was performed using the Rietveld method of full-profile crystal-structure analysis for polycrystalline samples [13] with derivative difference minimization refinement [14].

The specific heat data at temperatures ranging from 300 to 1073 K were calculated by the "ratio method" using a Netzsch STA Jupiter 449C differential scanning calorimeter equipped with a special sample holder for C_p measurements following the procedure reported in [12].

The thermal expansion was studied within the temperature range of 100−1000 K using a Netzsch Dil-402C inductive dilatometer in the dynamic regime at heating and cooling rates of 3−5 K/min. The measurements were performed in a dry helium flow (at 100−700 K) and "in air" (at 300−1000 K).

The specific volume and the unit cell parameters measured at room temperature are presented in the table. The X-ray diffraction analysis does not reveal any traces of uncontrolled impurities.

The detailed study of $GdCoO_3$ [12] indicates that the Curie constant C_{eff} and the Curie temperature Θ_{eff} in the expression $\chi_{Co} = N_A \dfrac{C_{eff}}{3k_B(T - \Theta_{eff})}$, where N_A is the Avogadro number and $2k_B$ is the Boltzmann constant, for the molar magnetic susceptibility of Co^{3+} ions depend on temperature. Both of them are related to the probability n_{HS} for charge carriers to occupy the high-spin state and to the width Δ_S of the spin gap as

$$C_{eff} = g^2\mu_B^2 S(S+1)n_{HS},$$
$$\Theta_{eff} = \frac{J_{Co-Co}zS(S+1)}{3k_B}n_{HS},$$

where

$$n_{HS} = \frac{g_{HS}\exp(-\Delta_S/k_BT)}{1 + g_{HS}\exp(-\Delta_S/k_BT)},$$
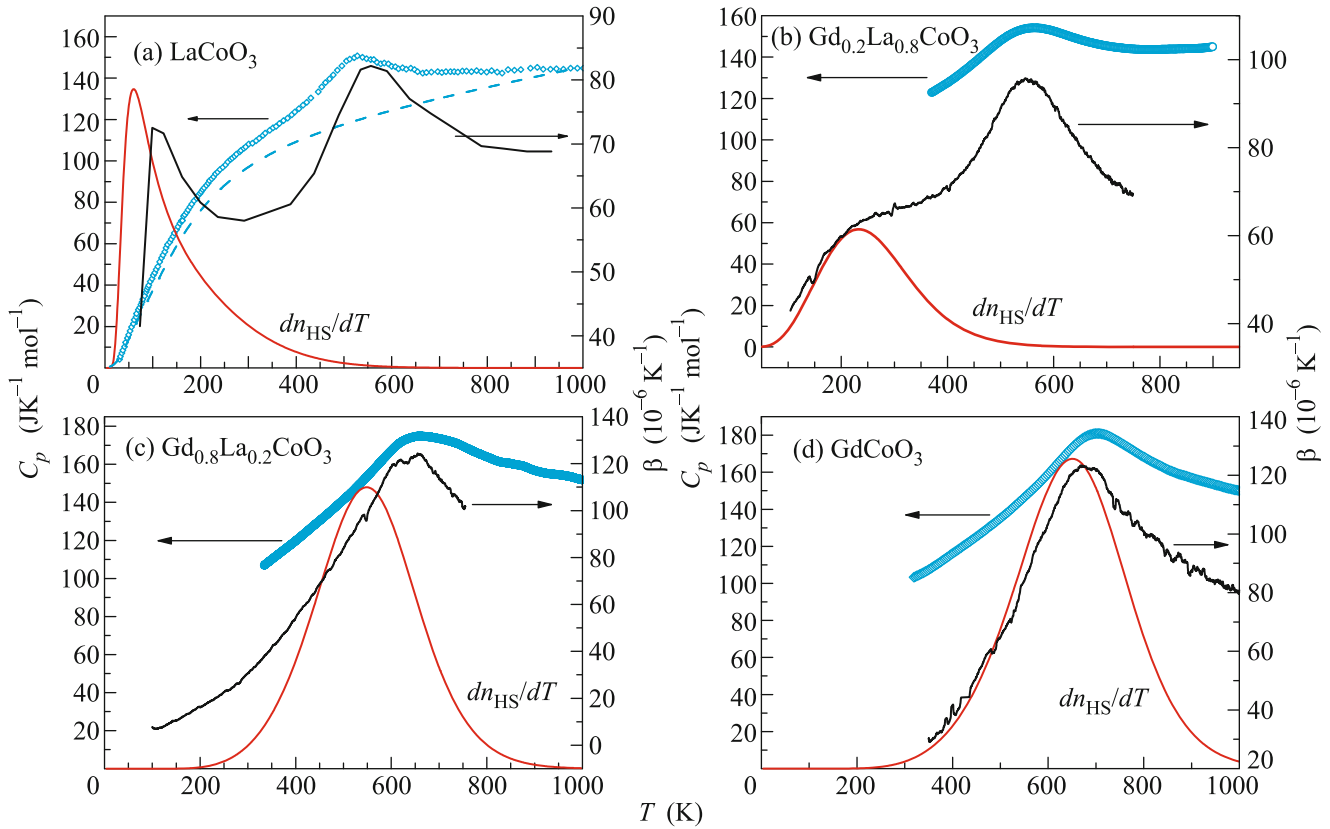
Fig. 1. (Color online) Measured temperature dependence of the molar specific heat and volume thermal expansion coefficient, as well as the calculated dn_{HS}/dT function characterizing the rate of filling for the high-spin state. The values of C_p and the thermal expansion coefficient β for LaCoO$_3$ are taken from [20, 21] and [10], respectively. For clarity, the values of dn_{HS}/dT are multiplied by the factors corresponding to the specific chemical compositions. The lattice specific heat is shown by the dashed line in Fig. 1a.

$g = 2$ is the purely spin Landé factor, μ_B is the Bohr magneton, $S = 2$ corresponds to the spin state of Co^{3+} ion, J_{Co-Co} is the exchange integral for a pair of cobalt ions, and $g_{HS} = 15$ is the degeneracy order of the $^5T_{2g}$ level. The explicit expression $\Delta_S(T) = \Delta_0[1 - (T/T_S)^n]$, where Δ_0 is the spin gap at $T = 0$ and T_S is the temperature at which the spin gap vanishes, for the spin gap [10] approximates well the results of the magnetic measurements with the parameters $\Delta_0 = 2300$ K, $T_S = 800$ K, and $n = 4$ for GdCoO$_3$ [12] and $\Delta_0 = 164$ K, $T_S = 230$ K, and $n = 2.97$ for LaCoO$_3$ [10]. The parameters Δ_0, n, and T_S for La$_{1-x}$Gd$_x$CoO$_3$ ($x = 0.2$, 0.5, 0.8) were determined in [15] by fitting the experimental data on the magnetic susceptibility. These data allowed us to calculate the temperature dependence $n_{HS}(T)$ for the population of high-spin states in the compounds under study and to plot the dn_{HS}/dT curves (Fig. 1). To compare the positions of peaks, the values of dn_{HS}/dT were multiplied by the corresponding factors.

The measured temperature dependence of the volume thermal expansion coefficient β obtained on cooling and on heating is shown in Fig. 1. Appreciable hysteresis phenomena are not observed. A good agreement between several series of measurements is obtained. For the coefficient β in La$_{1-x}$Gd$_x$CoO$_3$ ($x = 0$, 0.2, 0.5), we observe two smeared anomalies (at low and high temperatures). Such anomalies were studied earlier in undoped LaCoO$_3$ [8, 10]. We can see that the low-temperature peak in the temperature dependence of the thermal expansion coefficient correlates with that in dn_{HS}/dT (Figs. 1a and 1b), indicating its relation to the transition of Co^{3+} ions from the low- to high-spin state. With the growth of the gadolinium content, both peaks move toward higher temperatures. At the same time, the first peak moves much faster and the peaks eventually merge at the doping level x between 0.5 and 0.8. We use the Birch–Murnaghan equation of state [16, 17] for estimating the additional chemical pressure following the method described in [18]. This pressure arises because of the lanthanide compression. We have obtained the "critical" value $P_C \sim 7$ GPa of such pressure, near which the low-temperature peak in the temperature dependence of the thermal expansion disappears. The correctness of such estimate for P_C is confirmed by the existence of the second peak in PrCoO$_3$ and NdCoO$_3$ and by its
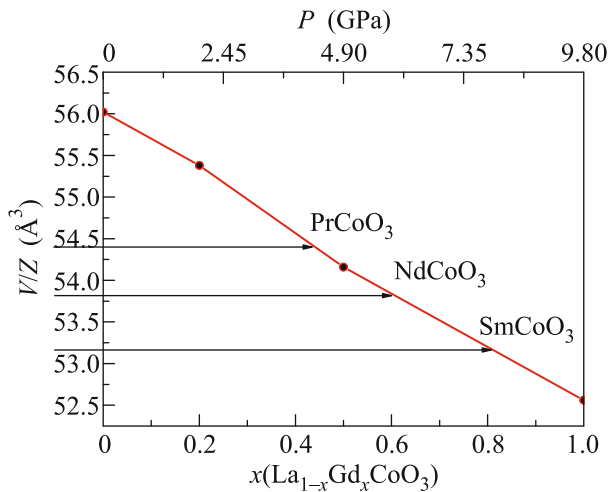
Fig. 2. (Color online) Unit cell volume for $La_{1-x}Gd_xCoO_3$ samples versus the doping level x and the corresponding values of the additional chemical pressure. The arrows indicate the unit cell volumes for $PrCoO_3$, $NdCoO_3$, and $SmCoO_3$. The measured values of the unit cell volume are shown by points and connected for clarity by the solid line.

absence in $SmCoO_3$ [9, 10]. The similar shift was observed earlier for the series of $La_{1-x}Eu_xCoO_3$ solid solutions [19]. In Fig. 2, we show the dependence of the unit cell volume in $La_{1-x}Gd_xCoO_3$ on the doping level x and the corresponding values of the additional chemical pressure.

The measured specific heat is illustrated in Fig. 1. We can see that the high-temperature anomalies, which are not related to the multiplicity fluctuations, turn out to be quite significant at high temperatures. To find the characteristics associated with these anomalies, we divide the molar specific heat for $La_{1-x}Gd_xCoO_3$ compounds into the regular component (the crystal lattice contribution) C_L and the anomalous contribution ΔC. To determine the contribution to the specific heat coming from the anharmonicity and free electrons, we use a linear combination of the Debye and Einstein functions supplemented by the linear term $C_L(T) = aC_D(T) + bC_E(T) + cT$. For fitting $C_L(T)$ to the results of measurements, we use the data reported in [20] for $LaCoO_3$ within the temperature range below 40 K and above 450 K, as well as the data for $YbCoO_3$ within the temperature range of 300–510 K [21], where the anomalous contribution to the specific heat is fairly small. The results for $C_L(T)$ are shown in Fig. 1a by the dashed line. The anomalous contributions for $La_{1-x}Gd_xCoO_3$ ($x = 0, 0.2, 0.5, 0.8, 1$) are illustrated in Fig. 3a. Naturally, the model under discussion is simplified and gives only a rough estimate for the anomalous specific heat and for the corresponding anomalous entropy.

In the $\Delta S(T)$ plots for $La_{1-x}Gd_xCoO_3$ (Fig. 3b), we can see two contributions to the entropy, which are
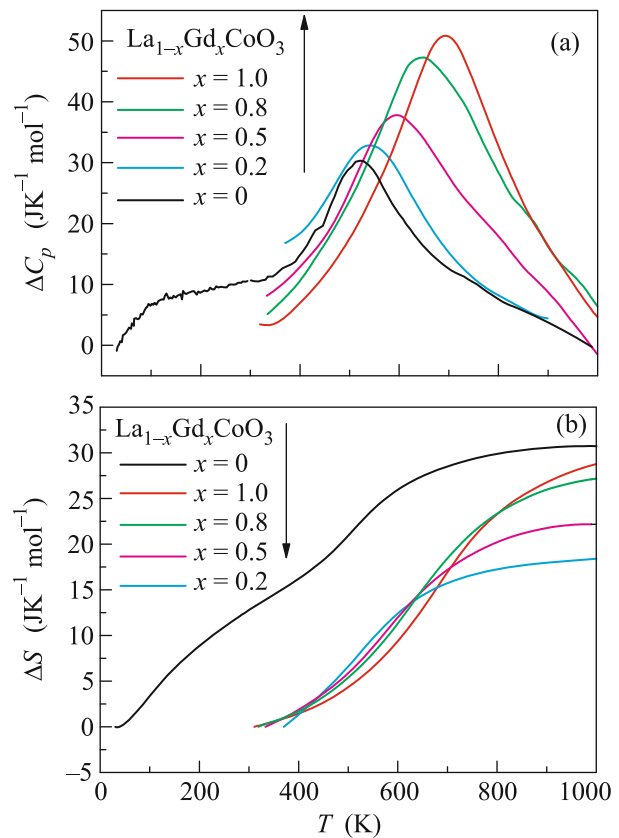

Fig. 3. (Color online) Temperature dependences of the anomalous specific heat $\Delta C(T)$ and of the anomalous contribution to the entropy $\Delta S(T)$ for $La_{1-x}Gd_xCoO_3$ ($x = 0$, 0.2. 0.5. 0.8, 1). For $LaCoO_3$, $\Delta C(T)$ and $\Delta S(T)$ are shown within the whole temperature range.

related to the changes in the spin and electron states, respectively. The entropy for the $La_{0.8}Gd_{0.2}CoO_3$ solid solution is close to that corresponding to the high-temperature anomaly in $LaCoO_3$; the entropy for $La_{0.5}Gd_{0.5}CoO_3$ has an intermediate value; i.e., the contribution from the low-temperature anomaly is observed; and the entropy for $La_{0.2}Gd_{0.8}CoO_3$ is close to the sum of entropies characteristic of the low- and high-temperature anomalies observed in undoped $LaCoO_3$ and $GdCoO_3$ compounds. Similar features can also be seen in the behavior of the total (Fig. 1) and anomalous (Fig. 3a) specific heats with the growth of the gadolinium content in $La_{1-x}Gd_xCoO_3$.

The specific heat at constant pressure is the derivative of enthalpy $W = E + PV$ with respect to the temperature: $C_p = \left.\dfrac{\partial W}{\partial T}\right|_P$. The internal energy can be represented in the form $E(T) = n_{HS}(T)E_{HS}(T) + n_{LS}(T)E_{LS}(T)$, where n_{HS} and n_{LS} are the populations of the high-spin (HS) and low-spin (LS) states, respectively, and E_{HS} and E_{LS} are the energies of these states. Since $n_{LS} = 1 - n_{HS}$, we find that $E(T) = E_{LS}(T) +$

$n_{HS}(T)\Delta_S(T)$, where $\Delta_S(T) = E_{HS}(T) - E_{LS}(T)$ is the so-called spin gap (the energy difference between the HS and LS states). Similarly, the specific volume is $V(T) = V_{LS}(T) + n_{HS}\Delta V(T)$, where $\Delta V(T) = V_{HS}(T) - V_{LS}(T)$. Therefore, the expressions for the enthalpy and specific heat have the form $W = E_{LS} + n_{HS}\Delta_S + PV_{LS} + Pn_{HS}\Delta V = W_{LS} + n_{HS}(\Delta_S + P\Delta V)$ and $C_p = \left.\dfrac{\partial W_{LS}}{\partial T}\right|_P + \dfrac{\partial n_{HS}}{\partial T}(\Delta_S + P\Delta V) + n_{HS}\left(\dfrac{\partial \Delta_S}{\partial T} + P\dfrac{\partial \Delta V}{\partial T}\right)$.

Here, $\left.\dfrac{\partial W_{LS}}{\partial T}\right|_P = C_p^{LS}$ is the specific heat of the system in the LS state, which can be treated as a certain background value. Cobalt ions in different spin states have different radii ($r_{HS} > r_{LS}$); therefore, the volume change with temperature $\Delta V(T)$ can be written as the sum of two contributions. The first contribution is due to the change in the unit cell volume related to the spin-state transition in the system of transition metal ions and the second one comes from the thermal expansion of the crystal lattice or the anharmonicity:

$$\Delta V = V_{HS}^{(0)}(1 + \beta_{HS}T) - V_{LS}^{(0)}(1 + \beta_{LS}T) = \Delta V_0 + T(\beta_{HS}V_{HS}^{(0)} - \beta_{LS}V_{LS}^{(0)}),$$

where $V_{HS}^{(0)}$ and $V_{LS}^{(0)}$ are the unit cell volumes at zero temperature corresponding to the HS and LS states, respectively, and β_{HS} and β_{LS} are the thermal expansion coefficients. As a result, we have

$$\dfrac{\partial \Delta V}{\partial T} = \beta_{HS}V_{HS}^{(0)} - \beta_{LS}V_{LS}^{(0)} \text{ and } C_p - C_p^{LS} = \dfrac{\partial n_{HS}}{\partial T}(\Delta S + P\Delta V) + n_{HS}\left[\dfrac{\partial \Delta_S}{\partial T} + P(\beta_{HS}V_{HS}^{(0)} - \beta_{LS}V_{LS}^{(0)})\right].$$

At atmospheric pressure, we can neglect the terms proportional to pressure. In this approximation, we have $C_p - C_p^{LS} \approx \dfrac{\partial n_{HS}}{\partial T}\Delta_S + n_{HS}\dfrac{\partial \Delta_S}{\partial T}$, i.e., the contribution related to the population of the HS state. On heating, all rare earth cobalt oxides and their solid solutions undergo a smooth insulator–metal transition. The additional electron contribution to the specific heat can be approximately written as $C_e \sim \dfrac{\partial}{\partial T}\left(\dfrac{E_g(T)}{e^{E_g(T)/2kT} + 1}\right)$, where $E_g(T)$ is the energy gap in the insulating state. Earlier, in [12, 15], we calculated the temperature dependences $E_g(T)$ and $\Delta_S(T)$ for several rare earth cobaltites. In Fig. 4, we show the temperature dependence for the sum of two contributions $(C_p - C_p^{LS}) + C_e$ for (a) LaCoO$_3$, (b) La$_{0.8}$Gd$_{0.2}$CoO$_3$, and (c) GdCoO$_3$. We can see that the growth in the gadolinium content leads to a shift to higher temperatures of the low-temperature feature in the specific heat $C_p - C_p^{LS}$ associated with the thermally driven population of the HS state. The shift occurs owing to the decrease in the spin gap. Then, both contributions to the specific heat gradually merge.
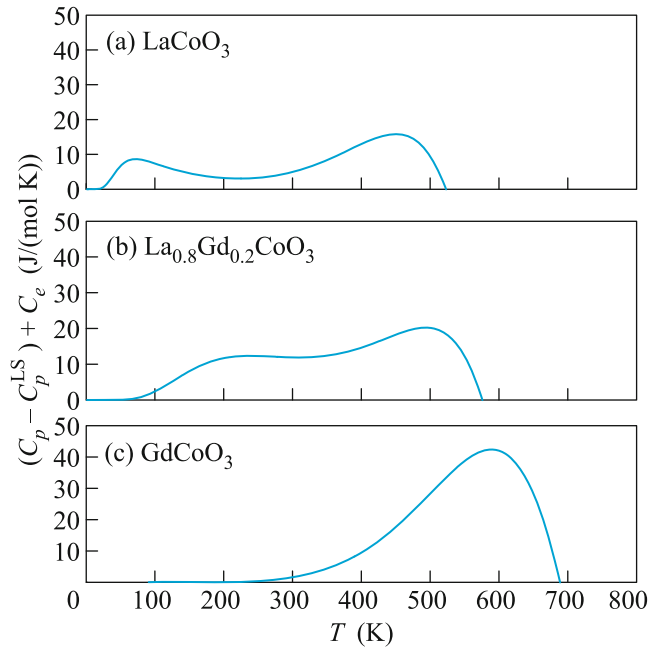
Fig. 4. (Color online) Temperature dependence of two features in the specific heat for (a) LaCoO$_3$, (b) La$_{0.8}$Gd$_{0.2}$CoO$_3$, and (c) GdCoO$_3$.

The combined analysis of the specific heat and thermal expansion of rare earth cobalt oxides and their solid solutions demonstrate that their temperature dependence exhibits characteristic anomalies related to the filling of the high-spin states of cobalt ions and to the additional electron contribution arising at the insulator–metal transition occurring with the growth of the temperature. With the decrease in the radius of the rare earth ion or with the growth of chemical pressure, the spin gap in these compounds grows and we observe the shift of the low-temperature feature toward higher temperatures and the gradual merging of the two contributions to the specific heat. For the whole LnCoO$_3$ series, the pressure dependence of the spin gap is presented in Fig. 3 in [18]. For lanthanides heavier than Gd, the spin gap exceeds 2000 K and achieves a value as high as 3700 K for Lu. This explains the stabilization of the low-spin state of cobalt ions and the absence of low-temperature anomalies in the magnetic and thermal characteristics. The calculations of the specific heat discussed above qualitatively interpret the behavior of two features in the temperature dependence observed in experiment, thus supporting our conclusions. The combined analysis of the new experimental data on the thermal expansion and specific heat of La$_{1-x}$Gd$_x$CoO$_3$ solid solutions and the corresponding calculations taking into account the contributions coming from the multiplicity fluctuations and metallization presented in this paper provides an opportunity to get a good insight into the mechanisms underlying the absence of two peaks in

thermal characteristics of the rare earth cobaltites with heavy lanthanides.

REFERENCES

1. C. R. Michel, A. H. Martinez, F. Huerta-Villalpando, and J. P. Moran-Lazaro, J. Alloys Compd. **484**, 605 (2009).

2. T. Inagaki, K. Miura, H. Yoshida, R. Maric, S. Ohara, X. Zhang, K. Mukai, and T. Fukui, J. Power Sources **86**, 347 (2000).

3. C. H. Chen, H. J. M. Bouwmeester, R. H. E. van Doorn, H. Kruidhof, and A. J. Burggraaf, Solid State Ionics **98**, 7 (1997).

4. N. B. Ivanova, S. G. Ovchinnikov, M. M. Korshunov, I. M. Eremin, and N. V. Kazak, Phys. Usp. **52**, 789 (2009).

5. I. O. Troyanchuk, D. V. Karpinskii, A. N. Chobot, and V. M. Dobryanskii, JETP Lett. **84**, 151 (2006).

6. I. O. Troyanchuk, A. N. Chobot, N. V. Tereshko, D. V. Karpinskii, V. Efimov, and V. Sikolenko, J. Exp. Theor. Phys. **112**, 837 (2011).

7. S. V. Vonsovskii and M. S. Svirskii, Sov. Phys. JETP **20**, 914 (1965).

8. P. G. Radaelli and S.-W. Cheong, Phys. Rev. B **66**, 094408 (2002).

9. K. Berggold, M. Kriener, P. Becker, M. Benomar, M. Reuther, C. Zobel, and T. Lorenz, Phys. Rev. B **78**, 134402 (2008).

10. K. Knizek, J. Jirak, J. Hejtmanek, M. Veverka, M. Marysko, G. Maris, and T. T. M. Palstra, Eur. Phys. J. B **47**, 213 (2005).

11. H. Hashimoto, T. Kusunose, and T. Sekino, Mater. Trans. **51**, 404 (2010).

12. Yu. S. Orlov, L. A. Solovyov, V. A. Dudnikov, A. S. Fedorov, A. A. Kuzubov, N. V. Kazak, V. N. Voronov, S. N. Vereshchagin, N. N. Shishkina, N. S. Perov, K. V. Lamonova, R. Yu. Babkin, Yu. G. Pashkevich, A. G. Anshits, and S. G. Ovchinnikov, Phys. Rev. B **88**, 235105 (2013).

13. H. M. Rietveld, J. Appl. Crystallogr. **2**, 65 (1969).

14. L. A. Solovyov, J. Appl. Crystallogr. **37**, 743 (2004).

15. S. G. Ovchinnikov, Yu. S. Orlov, V. A. Dudnikov, S. N. Vereshchagin, and N. S. Perov, J. Magn. Magn. Mater. **383**, 162 (2015).

16. F. J. Birch, Phys. Rev. **71**, 809 (1947).

17. F. J. Birch, J. Geophys. Res. **91**, 4949 (1986).

18. V. A. Dudnikov, S. G. Ovchinnikov, Yu. S. Orlov, N. V. Kazak, C. R. Michel, G. S. Patrin, and G. Yu. Yur'ev, J. Exp. Theor. Phys. **114**, 841 (2012).

19. J. Baier, S. Jodlauk, M. Kriener, A. Reichl, C. Zobel, H. Kierspel, A. Freimuth, and T. Lorenz, Phys. Rev. B **71**, 014443 (2005).

20. S. Stolen, F. Gronvold, and H. Brinks, Phys. Rev. B **55**, 14103 (1997).

21. M. Tachibana, T. Yoshida, H. Kawaji, T. Atake, and E. Takayama-Muromachi, Phys. Rev. B **77**, 094402 (2008).